Magma-induced axial subsidence during final-stage rifting: Implications for the development of seaward-dipping reflectors

Giacomo Corti[1], Andrea Agostini[2], Derek Keir[3], Jolante Van Wijk[4], Ian D. Bastow[5], and Giorgio Ranalli[6]

[1]*Consiglio Nazionale delle Ricerche, Istituto di Geoscienze e Georisorse, Via G. La Pira, 4, 50121 Florence, Italy*
[2]*Dipartimento di Scienze della Terra, Università degli Studi di Firenze, Via G. La Pira, 4, 50121 Florence, Italy*
[3]*National Oceanography Centre Southampton, University of Southampton, Southampton SO14 3ZH, United Kingdom*
[4]*Earth and Environmental Science Department, New Mexico Institute of Mining and Technology, 801 Leroy Place, Socorro, New Mexico 87801, USA*
[5]*Department of Earth Science and Engineering, Imperial College London, South Kensington Campus, London SW7 2AZ, United Kingdom*
[6]*Department of Earth Sciences and Ottawa-Carleton Geoscience Centre, Carleton University, Ottawa K1S 5B6, Canada*

ABSTRACT

A consensus is emerging from studies of continental rifts and rifted margins worldwide that significant extension can be accommodated by magma intrusion prior to the development of a new ocean basin. However, the influence of loading from magma intrusion, lava extrusion, and sedimentation on plate flexure and resultant subsidence of the basin is not well understood. We address this issue by using three-dimensional flexural models constrained by geological and geophysical data from the Main Ethiopian Rift and the Afar Depression in East Africa. Model results show that axial mafic intrusions in the crust are able to cause significant downward flexure of the opening rift and that the amount of subsidence increases with decreasing plate strength accompanying progressive plate thinning and heating during continental breakup. This process contributes to the tilting of basaltic flows toward the magma injection axis, forming the typical wedge-shaped seaward-dipping reflector sequences on either side of the eventual rupture site as the new ocean basin forms.

INTRODUCTION

During continental rifting the extending continental lithosphere is progressively modified by magmatic processes and mechanical deformation until it breaks and gives rise to new oceanic lithosphere bordered by young rifted continental margins. Although Earth materials are weak in extension, cratonic lithosphere retains significant strength during rifting, as evidenced in rift flank uplift and flexural isostasy studies of active rifts (e.g., Weissel and Karner, 1989; Ebinger et al., 1989). Progressive extension and plate thinning cause decompression melting of the asthenosphere at progressively shallower depths, leading to an increase in magma production through time (e.g., White and McKenzie, 1989; Buck, 2006), primarily focused in axial volcanic segments that mark the new plate boundary (e.g., Barberi and Varet, 1977; Ebinger and Casey, 2001; Wright et al., 2006). The sustained emplacement of the new magma into a narrow zone of the lithosphere and eruption at the surface modify the plate density profile, causing significant internal and surface loading. These loads promote plate flexure along the long and narrow intrusion zones, and change the state of stress within the plate (Beutel et al., 2010). Despite the importance of magmatism during late-stage rifting and continental breakup, the influence of loading from magma intrusion, lava extrusion, and sedimentation on plate flexure and resultant subsidence of the basin is not well understood. In this paper we describe flexural models that quantify the effect of axial intrusion and surface volcanism on basin subsidence within volcanic rifts, and demonstrate the increasing role of magmatic loading with progressive plate thinning and weakening. Extensional stresses induced by the plate bending beneath the volcanic load may facilitate the rise of magma from the mantle. These models are parameterized from seismic imaging, gravity surveys, and studies of plate strength (elastic thickness of the lithosphere) of the Main Ethiopian Rift (MER) and the Afar Depression in East Africa (Fig. 1), which represent unique modern-day analogs for processes occurring during continental breakup. The East African Rift zone is one of the few locations on Earth where the rift inception to rupture progression can be analyzed (e.g., Hayward and Ebinger, 1996; Bastow and Keir, 2011).

TECTONIC SETTING

The MER and Afar Depression formed as a result of the divergence of the Nubian, Somalian, and Arabian plates (Fig. 1) above an anomalously hot (e.g., Rooney et al., 2012; Ferguson et al., 2013), slow-seismic-wave-speed mantle (Montelli et al., 2004; Benoit et al., 2006; Bastow et al., 2005, 2008). Three plates interact within the Afar Depression, which comprises the subaerial Red Sea and Aden rifts and the northern termination of the MER. Whereas the MER opening is constrained to ~6 mm/yr, ~N100°E-directed motion between Nubia and Somalia (e.g., Bilham et al., 1999), both the Red Sea and Gulf of Aden systems show time-averaged extension rates of ~15–20 mm/yr related to the ~N35°E-oriented Africa-Arabia rifting (Fig. 1; e.g., Vigny et al., 2006; ArRajehi et al., 2010). These rates are augmented by discrete, large-volume dike intrusion events that accommodate decades to centuries of plate opening (e.g., Wright et al., 2012; Grandin et al., 2011). Geological, geodetic, and seismological measurements of active strain and magma intrusion across the Afro-Arabian rift zone show that south of ~16°N the rift bifurcates into two branches (the main Red Sea and the subaerial Red Sea rift in Afar), with an along-strike partitioning of extension. North of ~16°N, extension is within the main Red Sea Rift, whereas moving south of 16°N, extension is accommodated progressively on land within the Afar Depression (McClusky et al., 2010).
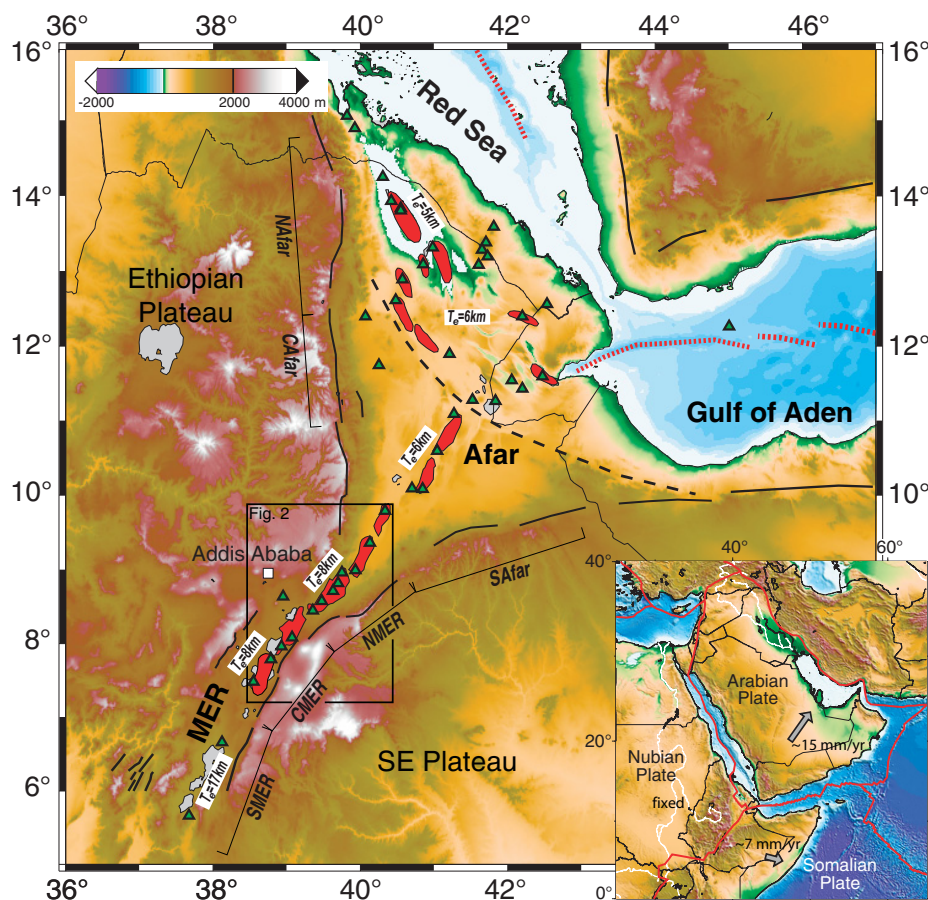
Figure 1. Tectonic setting of the Main Ethiopian Rift (MER) and Afar Depression (modified from Keir et al., 2013). Solid black lines show Oligocene–Miocene border faults of the Red Sea, Gulf of Aden, and East African rifts. Red segments show the Pleistocene–Holocene subaerial rift axes, and green triangles show Holocene volcanoes. Dashed lines show the Tendaho–Goba'ad discontinuity. Thick red dotted lines indicate ridge axes. Variations in the elastic thickness of the lithosphere (T_e) in the southern, central and northern MER (SMER, CMER, NMER, respectively) and in southern, central, and northern Afar (SAfar, CAfar, NAfar, respectively) are shown. Rift zone definitions are after Hayward and Ebinger (1996). Bottom right inset shows topography of northeast Africa and Arabia. Gray arrows show plate motions relative to a fixed Nubian plate (ArRajehi et al., 2010).

Geological and geophysical data show that the MER-Afar system opened by faulting and magmatism, with along-rift variations in style of extension interpreted as the expression of different stages in an evolutionary rift sequence (e.g., Hayward and Ebinger, 1996; Keir et al., 2013). The crustal thickness decreases from >35 km beneath the southern-central MER to <15 km in northern Afar (e.g., Makris and Ginzburg, 1987; Dugda et al., 2005; Stuart et al., 2006; Hammond et al., 2011), concomitant with a decrease in elastic thickness of the lithosphere from >15 km in the southern-central MER to ~5 km in northern Afar (Fig. 1; Hayward and Ebinger, 1996; Pérez-Gussinyé et al., 2009). The seismogenic layer thicknesses show a similar decrease from ~15 km in the MER (Keir et al., 2006) to ~5–7 km in northern Afar (Ayele et al., 2007; Nobile et al., 2012). Coincident with crustal thinning, geophysical and geological data indicate a northward increase in the volume of mafic magmatic intrusions and extrusive volcanism, which is also associated with a reduction in the elevation of the rift floor from ~1700 m above sea level in the southern-central MER to below sea level in the Danakil Depression of northern Afar (e.g., Bastow and Keir, 2011; Keir et al., 2013). Whereas in the southern-central MER extension is mostly accommodated through tectonic faulting at rift margins, in the northern MER and Afar strain migrated in the past 3–7 m.y. from Oligocene and Miocene border faults to ~15-km-wide, 60-km-long axial zones of localized faulting and magmatism, where magma intrusion plays a larger role than faulting in strain accommodation (e.g., Ebinger and Casey, 2001; Wolfenden et al., 2005; Ebinger et al., 2013). Geophysical data suggest that as much as 50% of the crust beneath the axial zones of localized faulting and magma intrusion is new igneous material. Crustal tomography reveals the presence of anomalously fast, elongate bodies in the middle to lower crust extending along the rift axis as shallow as ~10 km (Fig. 2; Keranen et al., 2004; Daly et al., 2008). These 20-km-wide and 50-km-long bodies are interpreted to represent cooled mafic intrusions (Keranen et al., 2004; Daly et al., 2008) containing at least 40% gabbro (Cornwell et al., 2006). The lateral variations in crustal properties and the presence of magmatic underplating make it difficult to unambiguously image the Moho across the rift. In this study we assume that the entire width of the rift extended by ~50%, and that the narrow magmatic segments approach 100% extension, primarily through the intrusion of new igneous crust through a process analogous to slow-spreading mid-ocean ridges (e.g., Iceland). The vertical and horizontal dimensions and density contrast of the large gabbroic bodies intruded into the crust during late-stage rifting have been interpreted to influence the vertical motions, state of stress, and architecture of the continental lithosphere (Keir et al., 2006; Beutel et al., 2010).

The data have been interpreted to indicate an along-axis variation in rift evolution, from embryonic rifting in the southern MER to incipient oceanic spreading in northern Afar (e.g., Hayward and Ebinger, 1996; Pagli et al., 2012), where Pleistocene–Holocene narrow axial basalt ranges (e.g., Erta Ale) are interpreted to be subaerial equivalents of oceanic spreading centers (e.g., Barberi and Varet, 1977). In the Danakil Depression of northern Afar, basalt flows from the axial ranges typically flow away into the lower lying, evaporite-rich basin (e.g., Pagli et al., 2012; Field et al., 2012), creating a thick (up to ~5 km) basin stratigraphy of thinly interbedded basalts and evaporites (Talbot, 2008), a geology typical of the seaward-dipping reflector sequences observed at volcanic rifted margins (e.g., Planke and Eldholm, 1994; White et al., 2008). Tilting of basaltic flows
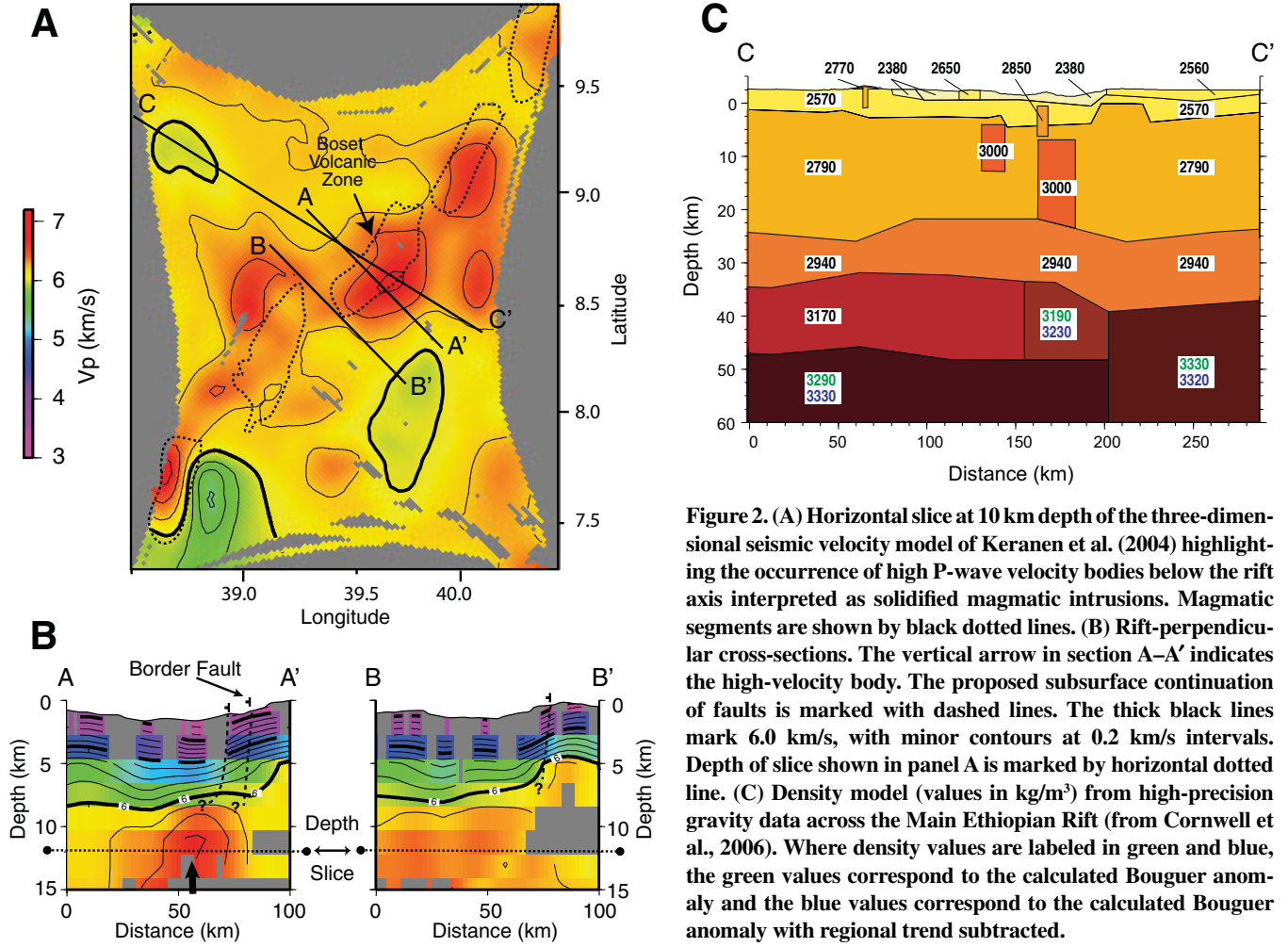
Figure 2. (A) Horizontal slice at 10 km depth of the three-dimensional seismic velocity model of Keranen et al. (2004) highlighting the occurrence of high P-wave velocity bodies below the rift axis interpreted as solidified magmatic intrusions. Magmatic segments are shown by black dotted lines. (B) Rift-perpendicular cross-sections. The vertical arrow in section A–A′ indicates the high-velocity body. The proposed subsurface continuation of faults is marked with dashed lines. The thick black lines mark 6.0 km/s, with minor contours at 0.2 km/s intervals. Depth of slice shown in panel A is marked by horizontal dotted line. (C) Density model (values in kg/m³) from high-precision gravity data across the Main Ethiopian Rift (from Cornwell et al., 2006). Where density values are labeled in green and blue, the green values correspond to the calculated Bouguer anomaly and the blue values correspond to the calculated Bouguer anomaly with regional trend subtracted.

toward the rift axis has been observed in other areas of Afar (e.g., Tendaho Graben and Manda Hararo Rift, Acocella et al., 2008; southeastern Afar margin in Djibouti, Le Gall et al., 2011), with structural features displaying striking similarities with those of coastal flexures creating seaward-dipping reflector sequences at volcanic rifted margins (Le Gall et al., 2011). Our study therefore provides important constraints on the initiation of seaward-dipping reflector sequences at magmatic margins.

FLEXURAL MODELS OF MAGMATIC LOADING

Model Setup

For the analysis of the vertical deflection due to a surface or subsurface load on an elastic plate overlying an inviscid substratum, we have used the numerical model by Li et al. (2004). The model is based on a high-order discretization with multigrid technique to solve the differential equation governing plate deflection, which is given by:

$$D\nabla^4 w(x,y) = -\left(\rho_m - \rho_{fill}\right)gw(x,y) + q(x,y), \quad (1)$$

where D is the flexural rigidity of an elastic plate, $w(x,y)$ is the vertical deflection of the plate, ρ_m is the density of mantle, ρ_{fill} is the density of the material occupying the space created by the flexural subsidence, and $q(x,y)$ is the net force per unit area exerted by the sum of applied loads:

$q(x,y) = \rho_{load}gh_{load}(x,y)$, where ρ_{load} and h_{load} are the density and thickness of the applied loads, respectively, and g is gravitational acceleration. The flexural rigidity D defines the resistance to bending of a continuous elastic plate:

$$D = \frac{ET_e^3}{12\left(1 - \upsilon^2\right)}, \quad (2)$$

where E is Young's modulus, υ is Poisson's ratio, and T_e is the effective elastic thickness of the plate; T_e represents the cumulative strength of a multilayered lithosphere to loading over the 10^4–10^5 yr time scales of isostasy. The model simulates reversible and instantaneous (purely elastic) deformation once the load is applied.

Although both the Afar Depression and the northern MER are highly faulted, the spatial dimensions of the magma intrusion zones and the geological characteristics of rifting justify the use of a thin, continuous plate model. Current deformation is largely accommodated at the rift axis, where the thinned lithosphere is strongly modified by the extensive magma intrusion and extension occurs through a combination of magmatic intrusion and faulting. The zones of active deformation show small offset faults that may have formed above dike intrusions (Rowland et al., 2007), and there is no structural or stratigraphic information for large offset normal faults within the narrow magmatic segments (e.g., Wolfenden et al., 2005; Rowland et al., 2007). The time and length scales of active and time-averaged deformation indicate that localized dike intrusion is more important in accommodating crustal strain over the past ~1 m.y. (e.g., Ebinger and

Casey, 2001; Wolfenden et al., 2005; Nobile et al., 2012; Ebinger et al., 2013). The border faults, both in Afar and the (northern) MER, are relatively inactive on the basis of seismic and field evidence, so that the faults are effectively locked at rift margins (e.g., Keir et al., 2006).

The three-dimensional (3D) model represents a plate with 250×250 cells, with a mesh size of 5×5 km^2; the load is applied on top of the continuous elastic plate (see Fig. 3). No initial topography of the bending plate (e.g., differences in elevation between the rift floor and the surrounding plateaus) was included in the models; this topography would simply be superimposed on the predicted plate bending. The following modeling results thus show the deformation as a result of the igneous load. A similar approach was used by Beutel et al. (2010) who studied deflection of two en echelon, rift segment–scale magma bodies (see discussion following).

The models are constrained by geophysical data of the tectonically active rift valleys of the MER zone. The values of T_e were varied between 4 km and 15 km, according to the northward reduction in T_e constrained by the gravity and topography coherence studies of Ebinger and Hayward (1996) (Fig. 1). Values of Young's modulus (70 GPa) and Poisson's ratio (0.30) were taken from Beutel et al. (2010). For the typical dimensions and densities of the axial intrusion we used constraints from controlled and passive source seismic tomography, models of magnetotelluric data, and 2D and 3D models of gravity data (Keranen et al., 2004; Tiberi et al., 2005; Cornwell et al., 2006; Whaler and Hautot, 2006; Daly et al., 2008) across axial magmatic segments in Ethiopia (Fig. 2). We used rectangular intrusions with 20 km width, 20–40 km length, and 10–16 km thickness, and a density contrast between the crust and the mafic intrusion of 210 kg/m^3 (Fig. 2C; Cornwell et al., 2006). The influence of the additional load imposed by synrift sedimentation was also considered: we used a density of 2380 kg/m^3 for the sedimentary rocks (Cornwell et al., 2006), which were considered to completely fill the depression resulting from the intrusion-related flexure. In addition, in some models we considered the external load imposed by the presence of volcanic edifices, whose dimensions were based on volcanoes from the northern MER (such as

Boseti: basal diameter 20 km, height 750 m, and volcanic rock density 2700–2900 kg/m^3).
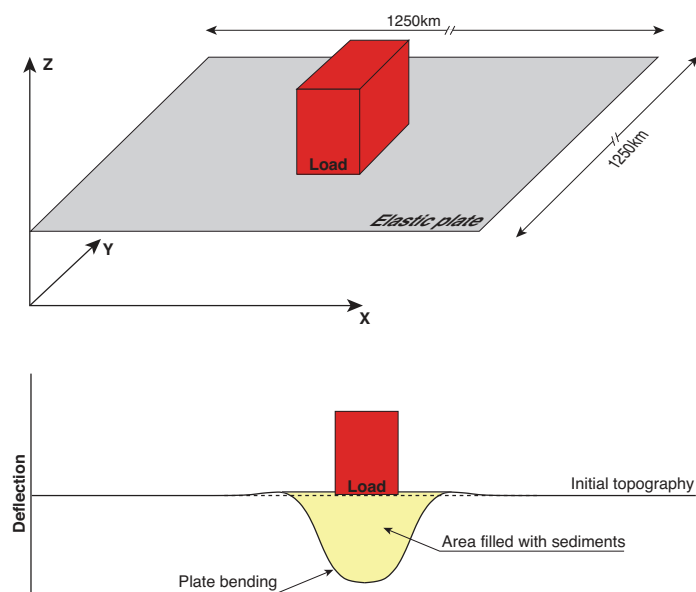
Results

We explored the deflection of the lithosphere induced by internal and external loading with varying plate thickness and size of magma intrusion both with and without synrift sedimentation (Figs. 4 and 5). The calculations show that the elastic plate bends in an ~100–150-km-wide region around the mafic intrusion zone with the amplitude of plate bending at a maximum above the center of the intrusions (Figs. 4A and 5). At the margins of the subsiding region, minor uplift (a few meters maximum) is observed, giving rise to a small forebulge as shown in Figure 5. The magnitude of the bending is primarily dependent on T_e (i.e., flexural thickness), the presence of synrift sediments, and the dimensions (i.e., volume) of the intrusions (Figs. 4B–4D).

The main control is exerted by variations in T_e, the decrease of which induces a prominent, nonlinear increase in plate bending: from ~200 m at T_e of 15 km, to ~400 m at T_e of 10 km, and to ~1000 m at T_e of 5 km (Fig. 4B). At all values of T_e, additional loading from synrift sediments approximately doubles the amount of subsidence (Fig. 4B). Increasing the length (Fig. 4C) or the thickness (Fig. 4D) of the intrusion also increases the subsidence. Our calculations demonstrate that the load of a volcanic edifice increases the amplitude of the plate bending, but its contribution beyond that created by the internal load is limited (typically <10%–20%), with the effect more pronounced at lower T_e and when the size of the magma intrusion is smaller (i.e., decreasing the internal load; Figs. 4B–4D). In addition, the presence of a volcanic edifice has a more limited influence on plate bending than that of the sedimentary infill, despite volcanic rocks having a higher density (2700 kg/m^3) than sediments (2380 kg/m^3), a result related to larger volume of the subsiding region filled by sedimentary rocks than that of the volcanic edifice. Comparison of plate bending in the case illustrated here of a single mafic intrusion with the case of two en echelon bodies (Beutel et al., 2010) shows no significant variation in subsidence, with differences never exceeding ~50 m (Fig. 6). Additional tests made with variations in density and height of the surface volcano suggest no significant influence of these parameters on plate bending.

The relation between the maximum subsidence w_0 and T_e is highly nonlinear and can be fit by a power function in the form $w_0 = A\,T_e^{-B}$, where A and B are parameters varying in the range 2.8–8.7 × 10^3 and 1.1–1.5, respectively, as a function of the variable load (presence of volcano, sediment infill, and length and thickness of the intrusion). This relation is of the same form as the dependence in the case of a line load ($w_0 = q_0 \alpha^3/8D$; i.e., $w_0 \sim A\,T_e^{-B}$, where q_0, α, and D are load, flexural parameter, and flexural rigidity, respectively, and $B = 3/4$; e.g., Turcotte and Schubert, 2002).

DISCUSSION AND IMPLICATIONS FOR THE DEVELOPMENT OF SEAWARD-DIPPING REFLECTORS

Data from continental rifts and rifted margins worldwide indicate that significant extension can be accommodated by magma intrusion prior to the development of a new ocean basin (e.g., Ebinger and Casey, 2001; Thybo and Nielsen, 2009; Bastow and Keir, 2011). The emplacement of large volumes of magma into the lithosphere (and eruption at the surface) modifies its density profile and transfers heat to the plate, affecting the patterns of long-term subsidence predicted by theoretical models of stretching and thinning of the continental lithosphere (e.g., Buck, 2004; Daniels et al., 2014). In particular, intrusion of large magma volumes in the lithosphere, as observed in the MER, may cause significant internal and surface loading resulting in plate flexure and rift subsidence (Beutel et al., 2010).

Figure 3. (Top) Three-dimensional setting of the models. (Bottom) Profile of lithospheric response to loading, showing the area filled with sediments (load not to scale).
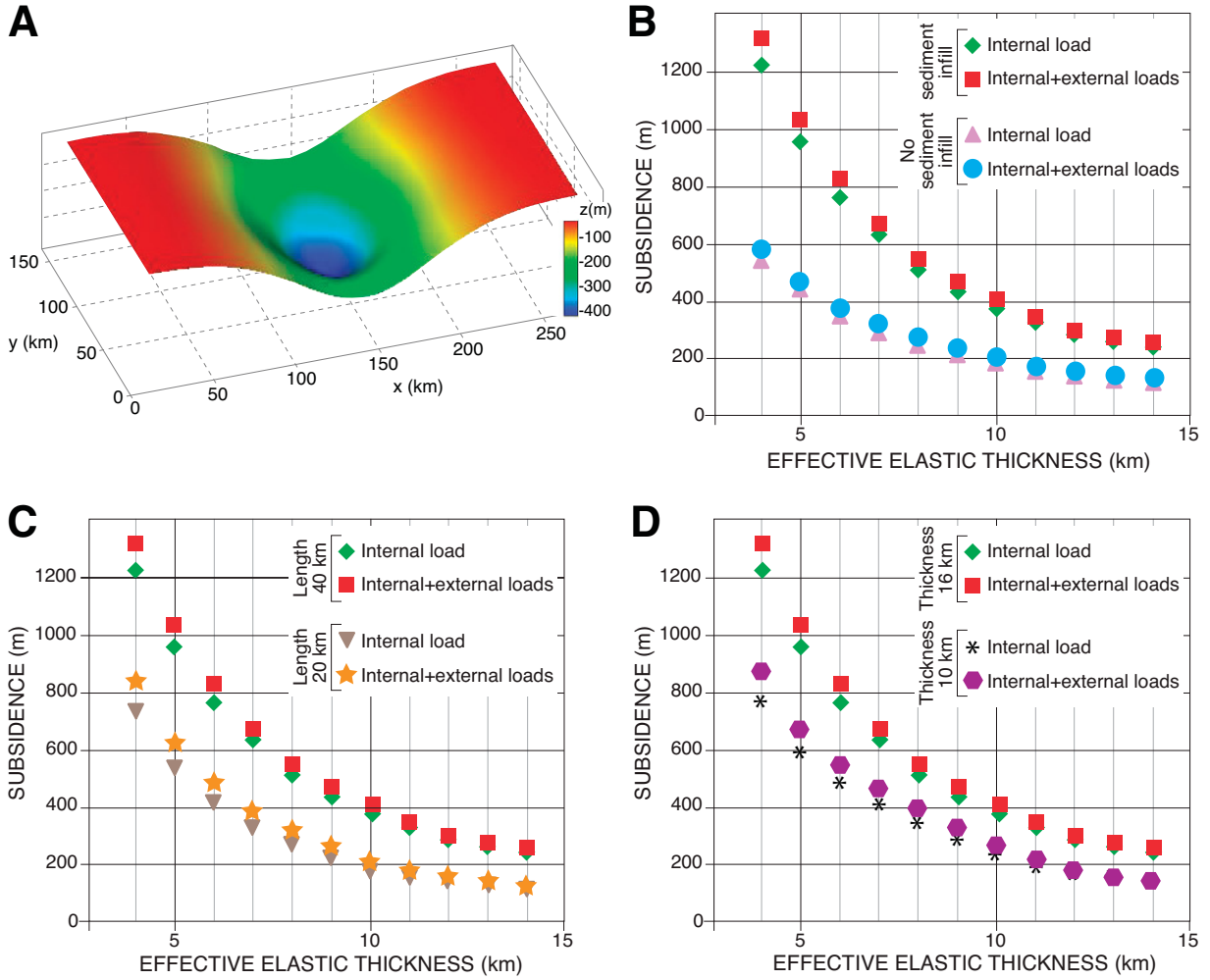
Figure 4. (A) Three-dimensional view of the typical plate bending resulting from crustal magma intrusion and volcanic loading. (B) Plot of maximum subsidence versus elastic thickness T_e for a single mafic intrusion (length 40 km, width 20 km, thickness 16 km) and variable sediment fill (present or absent). (C) Maximum subsidence versus T_e for variable length (width 20 km, thickness 16 km). (D) Maximum subsidence versus T_e for variable thickness (length 40 km, width 20 km) of the mafic intrusion. In all the plots calculations are reported for the cases where a surface volcano is absent (internal load only) or present (internal + external loads); in this latter case, the density of the volcano is assumed to be 2700 kg/m³. In C and D, all values are calculated with sediment infill.

Despite some inherent limitations (e.g., constant flexural rigidity and T_e throughout the model domain, simplified shape of the intrusions), our simple flexural models have allowed quantification of this process, significantly extending the previous state of stress studies by Beutel et al. (2010). Although not included in our continuous plate models of intruded loads and surface (volcano) loads, analytical and numerical models provide insights into the role of in-plane tensional stresses on the shapes of the plate deflection beneath the volcanic loads (e.g., ten Brink, 1991; Ebinger and Hayward, 1996). Assuming a tensional stress of 2×10^{12} Nm⁻¹ (e.g., Kusznir et al., 1991) applied to an 800-m-high line load on a plate with T_e of 10 km would reduce the maximum subsidence by ~12% and broaden the depression by ~25%. Our results, therefore, are probably overestimates of the maximum subsidence.

The results show a nonlinear increase in amount of subsidence when T_e decreases, with the implication that as the plate weakens during progressive thinning and heating during riftin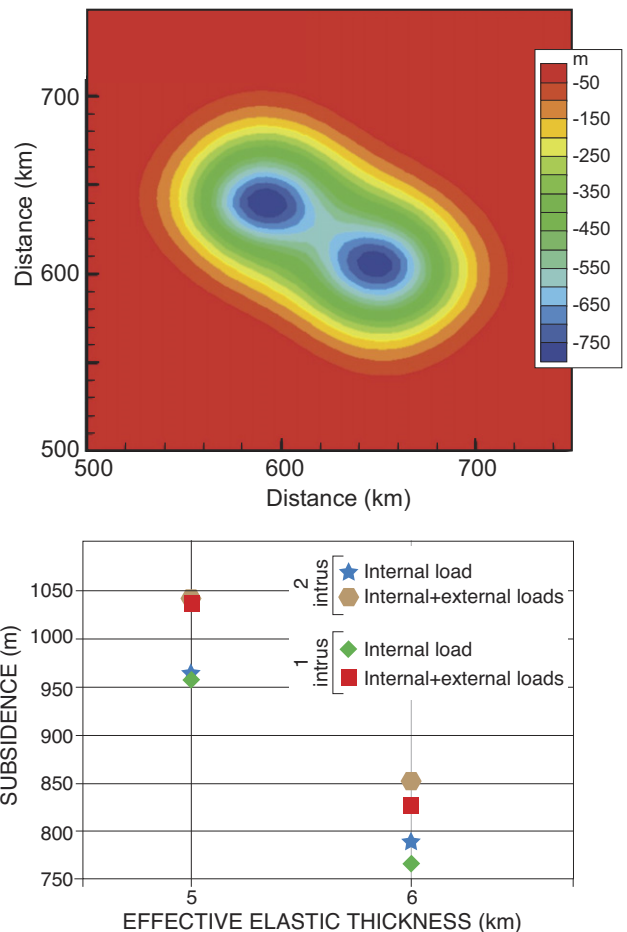g, loading-induced subsidence will become an increasingly important mechanism driving rift evolution. In the MER, where T_e is typically >8–10 km, the effect of the large mafic intrusions imaged by geophysical data is relatively small (Beutel et al., 2010). However, thickening of the youngest sediments above the axial intrusions is suggested by the geometry of the low-velocity upper crustal layers imaged in seismic tomography by Keranen et al. (2004; see Fig. 2B): the uppermost units thicken dramatically directly above the intrusions, in contrast to deeper units that have a more uniform thickness across the rift. In addition, bending of the rift floor is visible in topographic profiles across magmatic segments, such as along a profile from the Asela-Langano boundary fault system into the Aluto-Gedemsa magmatic segment (Pizzi et al., 2006). Although the overall riftward bending may result from initial (Miocene) phases of basin downwarping (e.g., Zanettin and Justin-Visentin, 1975; Kazmin et al., 1980), the architecture of recent (Pliocene–Pleistocene) rift-related sediments (e.g., riftward tilting of Pleistocene–Holocene alluvial fans) at the eastern (Asela-Langano) margin (see Agostini
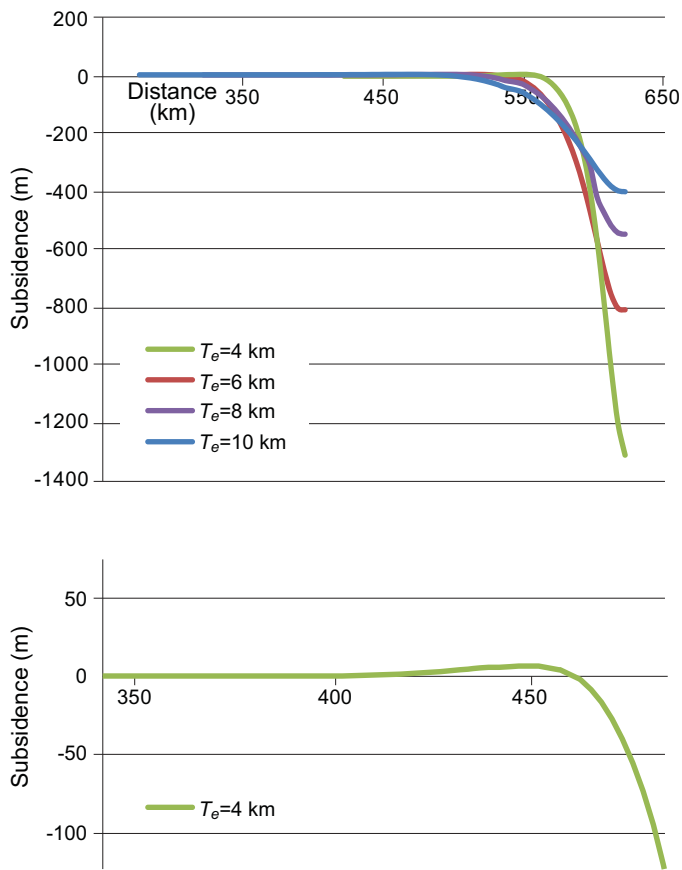
Figure 5. (Top) **Profile showing plate deflection perpendicular to the long axis of the intrusion for different elastic thickness T_e (values calculated with internal + external loads and sediment infill; dimensions of intrusions: length 40 km, width 20 km, thickness 16 km). (Bottom) Close-up of the model with T_e = 4 km showing a minor uplift giving rise to a forebulge at the margin of the subsiding region (maximum uplift is ~5 m).**

Figure 6. (Top) **Two-dimensional view of plate bending related to the presence of two en echelon intrusions (modified from Beutel et al., 2010). (Bottom) Plot of maximum subsidence versus elastic thickness T_e for a single or two intrusions (intrus) and variable loading (internal load only or internal + external loads). Values are calculated with sediment infill. Dimensions of intrusions: length 40 km, width 20 km, thickness 16 km.**

et al., 2011) points toward a recent tilting likely induced by axial magma intrusion (see also Pizzi et al., 2006; Fig. 7A).
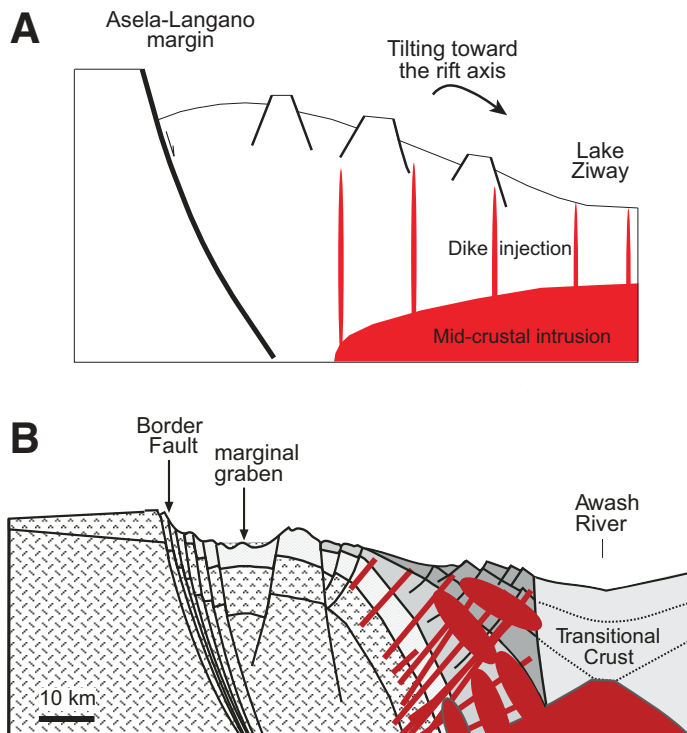
An overall bending of the rift toward axial zones of intensive dike intrusion and magmatic construction has been observed in the southern Red Sea rift (Fig. 7B; Wolfenden et al., 2005), as well as in other regions of central-southern Afar (e.g., Tendaho Graben and Manda Hararo Rift, Acocella et al., 2008; southeastern Afar margin in Djibouti, Le Gall et al., 2011), creating an axis-dipping wedge of primarily basaltic flows analogous to seaward-dipping reflector sequences imaged on volcanic margins worldwide (e.g., Eldholm et al., 1989; Planke and Eldholm, 1994). Intrusion-induced subsidence is expected to increase in northern Afar, where T_e decreases significantly to ~5 km in the Danakil Depression (Ebinger and Hayward, 1996). In this area, the basin floor reaches below sea level and is dominated by young evaporite-rich basins bisected by the basalt-rich Pleistocene–Holocene Erta Ale volcanic range. Here, an active axial intrusion shallower than ~10 km depth is modeled by InSAR (interferometric synthetic aperture radar) data (e.g., Amelung et al., 2000; Pagli et al., 2012; Nobile et al., 2012). Limited borehole data suggest that the basin is filled by 3 km or more of interbedded Pliocene–Holocene evaporites and basalt flows (Hutchinson and Engels, 1972), suggesting that rapid subsidence of

the region toward and below sea level accelerated during the past 5 m.y. Our models suggest that as much as 1 km of this subsidence (i.e., ~33%) is likely to be caused by the intrusion-related loading and plate flexure, which also accounts for the thickness of the basin fill. The remainder is caused by the response of the lithosphere to faulting and lithospheric thinning, as well as localized subsidence above dikes as an elastic response directly above the mode I opening at depth.

Loading of the lithosphere has been shown to create flexural stresses capable of controlling processes such as magma ascent and emplacement during extension and the spacing of volcanoes in rift settings; the load imposed by volcanic edifices has been considered the major parameter contributing to these flexural stresses (ten Brink, 1991). Our results, however, suggest that the contribution to subsidence by the load of a volcanic edifice is relatively small compared to the intrusion-induced subsidence. Our analysis indicates that volumetrically large crustal intrusions, rather than volcanoes, may have a strong control on rift morphology over time. The base of the bent plate will be in extension, facilitating the rise of magma, and serving to maintain the along-axis magma intrusion zones.
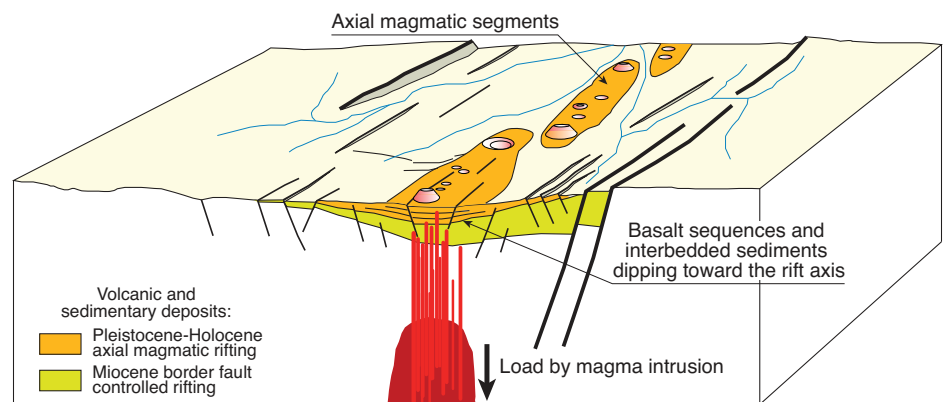
A Asela-Langano margin

Tilting toward the rift axis

Lake Ziway

Dike injection

Mid-crustal intrusion

B Border Fault

marginal graben

Awash River

Transitional Crust

10 km

Figure 7. (A) Sketch of the topography of the eastern margin of the central Main Ethiopian Rift at Asela-Langano showing tilting of fault blocks toward the rift axis, which may be induced by mid-crustal intrusion beneath the rift floor (modified from Pizzi et al., 2006). (B) Schematic cross section illustrating magmatic margin development of the southern Red Sea Rift (after Wolfenden et al., 2005). Riftward-dipping and offlapping basaltic flows form a riftward-dipping wedge analogous to seaward-dipping reflector sequences imaged on volcanic margins worldwide.

Figure 8 summarizes the general consequences of flexure caused by internal loads. After the initial phases of tectonic rifting, which may create asymmetric basins with depocenters in correspondence to the main boundary faults, strain migrates to axial zones of localized faulting and magma intrusion, where significant subsidence is initiated when large volumes of magma intrude the lithosphere and accommodate extension. Intrusion-related subsidence becomes an increasingly important mechanism driving increasing rift subsidence as the plate weakens during progressive rifting leading to the formation of new columns of hot weak lithosphere at nascent mid-ocean ridges. In the final stages of breakup, when thinning of the heavily intruded, weakened plate induces a pulse of decompression melting and a significant increase in extrusive magmatism (see also Nielsen and Hopper, 2004; Bastow and Keir, 2011), the axial intrusion-induced subsidence serves to progressively reorient the basalt sequences and interbedded sediments to dip toward the future breakup boundary. Consequently, subsidence caused by high-density crust at zones of intrusion is a factor in the reorientation of originally subhorizontal flows to form the seaward-dipping reflector sequences at the newly formed magmatic rifted margins as the rift breaks the continent and the rifted margins continue to subside below sea level while the heat transferred to the plate during rifting gradually dissipates (e.g., Wolfenden et al., 2005; Beutel et al., 2010; Bastow and Keir, 2011; Keir et al., 2013). Thus, this process may represent a contributing factor to the development of the seaward-dipping reflector sequences, which are normally interpreted as either resulting from progressive oceanward flexuring of the lavas due to differential loading by the newly erupted flows (isostatic models; e.g., Palmason, 1980; Mutter et al., 1982; Mutter, 1985; Eldholm, 1991) or tectonic features associated with fault development (e.g., fault-related flexures controlled by major continentward-dipping normal faults; e.g., Nielsen, 1975; Tard et al., 1991; Barton and White, 1997; Geoffroy et al., 1998; Geoffroy, 2005; Quirk et al., 2014).

Figure 8. Three-dimensional sketch showing flexure of the crust resulting from high-density magmatic intrusions emplaced within the magmatic segments. Deposition of early rift sediments is controlled by major boundary faults that cause wedging toward the most active rift margin (e.g., Wolfenden et al., 2004). Later deposition is instead influenced by magma intrusion at the break-up axis, which results in progressive tilting of interbedded sedimentary and volcanic layers, giving rise to a dominantly seaward-dipping pattern of reflectors, as observed on magma-dominated rifted margins (modified from Keir et al., 2006; Beutel et al., 2010).

Axial magmatic segments

Basalt sequences and interbedded sediments dipping toward the rift axis

Volcanic and sedimentary deposits:
Pleistocene-Holocene axial magmatic rifting
Miocene border fault controlled rifting

Load by magma intrusion

REFERENCES CITED

Acocella, V., Abebe, B., Korme, T., and Barberi, F., 2008, Structure of Tendaho Graben and Manda Hararo Rift: Implications for the evolution of the southern Red Sea propagator in central Afar: Tectonics, v. 27, TC4016, doi:10.1029/2007TC002236.

Agostini, A., Bonini, M., Corti, G., Sani, F., and Manetti, P., 2011, Distribution of Quaternary deformation in the central Main Ethiopian Rift, East Africa: Tectonics, v. 30, TC4010, doi:10.1029/2010TC002833.

Amelung, F., Oppenheimer, C., Segall, P., and Zebker, H., 2000, Ground deformation near Gada 'Ale Volcano, Afar, observed by radar interferometry: Geophysical Research Letters, v. 27, p. 3093–3096, doi:10.1029/2000GL008497.

ArRajehi, A., and 16 others, 2010, Geodetic constraints on present-day motion of the Arabian Plate: Implications for Red Sea and Gulf of Aden rifting: Tectonics, v. 29, TC3011, doi: 10.1029/2009TC002482.

Ayele, A., Stuart, G., Bastow, I., and Keir, D., 2007, The August 2002 earthquake sequence in north Afar: Insights into the neotectonics of the Danakil microplate: Journal of African Earth Sciences, v. 48, p. 70–79, doi:10.1016/j.jafrearsci.2006.06.011.

Barberi, F., and Varet, J., 1977, Volcanism of Afar: Small-scale plate tectonics implication: Geological Society of America Bulletin, v. 88, p. 1251–1266, doi:10.1130/0016-7606 (1977)88<1251:VOASPT>2.0.CO;2.

Barton, A.J., and White, R.S., 1997, Volcanism on the Rockall continental margin: Geological Society, London, Journal, v. 154, p. 531–536, doi:10.1144/gsjgs.154.3.0531.

Bastow, I., and Keir, D., 2011, The protracted development of the continent-ocean transition in Afar: Nature Geoscience, v. 4, p. 248–250, doi:10.1038/ngeo1095.

Bastow, I.D., Stuart, G.W., Kendall, J.M., and Ebinger, C.J., 2005, Upper mantle seismic structure in a region of incipient continental breakup: Northern Ethiopian rift: Geophysical Journal International, v. 162, p. 479–493, doi:10.1111/j.1365-246X.2005 .02666.x.

Bastow, I.D., Nyblade, A.A., Stuart, G.W., Rooney, T.O., and Benoit, M.H., 2008, Upper mantle seismic structure beneath the Ethiopian hot spot: Rifting at the edge of the African low-velocity anomaly: Geochemistry, Geophysics, Geosystems, v. 9, Q12022, doi: 10.1029/2008GC002107.

Benoit, M.H., Nyblade, A.A., Owens, T.J., and Stuart, G., 2006, Mantle transition zone structure and upper mantle S velocity variations beneath Ethiopia: Evidence for a broad, deep-seated thermal anomaly: Geochemistry, Geophysics, Geosystems, v. 7, Q11013, doi: 10.1029/2006GC001398.

Beutel, E., van Wijk, J., Ebinger, C., Keir, D., and Agostini, A., 2010, Formation and stability of magmatic segments in the Main Ethiopian and Afar rifts: Earth and Planetary Science Letters, v. 293, p. 225–235, doi:10.1016/j.epsl.2010.02.006.

Bilham, R., Bendick, R., Larson, K., Mohr, P., Braun, J., Tesfaye, S., and Asfaw, L., 1999, Secular and tidal strain across the Main Ethiopian Rift: Geophysical Research Letters, v. 26, p. 2789–2792, doi:10.1029/1998GL005315.

Buck, W.R., 2004, Consequences of asthenospheric variability on continental rifting, *in* Karner, G.D., et al., eds., Rheology and deformation of the lithosphere at continental margins: New York, Columbia University Press, p. 1–30.

Buck, W.R., 2006, The role of magma in the development of the Afro-Arabian Rift System, *in* Yirgu, G., et al., eds., The Afar Volcanic Province within the East African Rift System: Geological Society of London Special Publication 259, p. 43–54, doi:10.1144/GSL.SP .2006.259.01.05.

Cornwell, D.G., Mackenzie, G.D., England, R.W., Maguire, P.K.H., Asfaw, L., and Oluma, B., 2006, Northern main Ethiopian rift crustal structure from new high-precision gravity data, *in* Yirgu, G., et al., eds., The Afar Volcanic Province within the East African Rift System: Geological Society of London Special Publication 259, p. 307–321, doi: 10.1144/GSL.SP.2006.259.01.23.

Daly, E., Keir, D., Ebinger, C.J., Stuart, G.W., Bastow, I.D., and Ayele, A., 2008, Crustal tomographic imaging of a transitional continental rift: The Ethiopian rift: Geophysical Journal International, v. 172, p. 1033–1048, doi:10.1111/j.1365-246X.2007.03682.x.

Daniels, K.A., Bastow, I.D., Keir, D., Sparks, R.S.J., and Menand, T., 2014, Thermal models of dyke intrusion during the development of continent-ocean transition: Earth and Planetary Science Letters, v. 385, p. 145–153, doi:10.1016/j.epsl.2013.09.018.

Dugda, M., Nyblade, A., Julia, J., Langston, C., Ammon, C., and Simiyu, S., 2005, Crustal structure in Ethiopia and Kenya from receiver function analysis: Journal of Geophysical Research, v. 110, no. B1, doi:10.1029/2004JB003065.

Ebinger, C., and Casey, M., 2001, Continental breakup in magmatic provinces: An Ethiopian example: Geology, v. 29, p. 527–530, doi:10.1130/0091-7613(2001)029<0527:CBIMPA >2.0.CO;2.

Ebinger, C.J., and Hayward, N.J., 1996, Soft plates and hot spots: Views from Afar: Journal of Geophysical Research, v. 101, p. 21859–21876.

Ebinger, C.J., Bechtel, T.D., Forsyth, D.W. and Bowin, C.O., 1989, Effective elastic plate thickness beneath the East African and Afar plateaus and dynamic compensation of the uplifts: Journal of Geophysical Research, v. 94, p. 2883–2901, doi:10.1029 /JB094iB03p02883.

Ebinger, C.J., van Wijk, J., and Keir, D., 2013, The time scales of continental rifting: Implications for global processes, *in* Bickford, M.E., ed., The web of geological sciences: Advances, impacts, and interactions: Geological Society of America Special Paper 500, p. 371–396, doi:10.1130/2013.2500(11).

Eldholm, O., 1991, Magmatic-tectonic evolution of a volcanic rifted margin: Marine and Petroleum Geology, v. 102, p. 43–61, doi:10.1016/0025-3227(91)90005-O.

Eldholm, O., Thiede, J., and Taylor, E., 1989, Evolution of the Vøring volcanic margin, *in* Eldholm, O., et al., Proceedings of the Ocean Drilling Program, Scientific Results, Volume 104: College Station, Texas, Ocean Drilling Program, p. 1033–1065, doi:10.2973 /odp.proc.sr.104.191.1989.

Ferguson, D.J., Maclennan, J., Bastow, I.D., Pyle, D.M., Keir, D., Blundy, J.D., Plank, T., and Yirgu, G., 2013, Melting during late-stage rifting in Afar is hot and deep: Nature, v. 499, p. 70–73, doi:10.1038/nature12292.

Field, L., Barnie, T., Blundy, J., Brooker, R.A., Keir, D., Lewi, E., and Saunders, K., 2012, Integrated field, satellite and petrological observations of the November 2010 eruption of Erta Ale: Bulletin of Volcanology, v. 74, p. 2251–2271, doi:10.1007/s00445-012 -0660-7.

Geoffroy, L., 2005, Volcanic passive margins: Comptes Rendus Geoscience, v. 337, p. 1395–1408, doi:10.1016/j.crte.2005.10.006.

Geoffroy, L., Gelard, J.P., Lepvrier, C., and Olivier, P., 1998, The coastal flexure of Disko (West Greenland), onshore expression of the 'oblique reflectors': Geological Society, London, Journal, v. 155, p. 463–473, doi:10.1144/gsjgs.155.3.0463.

Grandin, R., Jacques, E., Nercessian, A., Ayele, A., Doubre, C., Socquet, A., Keir, D., Kassim, M., Lemarchand, A., and King, G.C.P., 2011, Seismicity during lateral dike propagation: Insights from new data in the recent Manda Hararo–Dabbahu rifting episode (Afar, Ethiopia): Geochemistry, Geophysics, Geosystems, v. 12, Q0AB08, doi:10.1029 /2010GC003434.

Hammond, J.O.S., Kendall, J.-M., Stuart, G.W., Keir, D., Ebinger, C., Ayele, A., and Belachew, M., 2011, The nature of the crust beneath the Afar triple junction: Evidence from receiver functions: Geochemistry, Geophysics, Geosystems, v. 12, Q12004, doi:10.1029 /2011GC003738.

Hayward, N., and Ebinger, C., 1996, Variations in the along–axis segmentation of the Afar rift system: Tectonics, v. 15, p. 244–257, doi:10.1029/95TC02292.

Hutchinson, R.W., and Engels, G.G., 1972, Tectonic evolution of the southern Red Sea and its possible significance to older rifted continental margins: Geological Society of America Bulletin, v. 83, p. 2989–3002, doi:10.1130/0016-7606(1972)83[2989:TEITSR]2.0.CO;2.

Kazmin, V., Seife, M.B., Nicoletti, M., and Petrucciani, C., 1980, Evolution of the northern part of the Ethiopian Rift, *in* Geodynamic Evolution of the Afro-Arabian Rift System: Accademia Nazionale Dei Lincei, Atti dei Convegni Lincei 47, p. 275–292.

Keir, D., Ebinger, C., Stuart, G., Daly, E., and Ayele, A., 2006, Strain accommodation by magmatism and faulting as rifting proceeds to breakup: Seismicity of the northern Ethiopian rift: Journal of Geophysical Research, v. 111, no. B5, p. B05314, doi:10.1029/2005JB003748.

Keir, D., Bastow, I.D., Pagli, C., and Chambers, E.L., 2013, The development of extension and magmatism in the Red Sea rift of Afar: Tectonophysics, v. 607, p. 98–114, doi: 10.1016/j.tecto.2012.10.015.

Keranen, K., Klemperer, S.L., Gloaguen, R., and EAGLE Working Group, 2004, Three-dimensional seismic imaging of a protoridge axis in the Main Ethiopian rift: Geology, v. 32, p. 949–952, doi:10.1130/G20737.1.

Kusznir, N.J., Vita-Finzi, C., Whitmarsh, R.B., England, P., Bott, M.H.P., Govers, R., Cartwright, J., and Murrell, S., 1991, The distribution of stress with depth in the lithosphere: Thermo-rheological and geodynamic constraints [and discussion]: Royal Society of London Philosophical Transactions, ser. A, v. 337, no. 1645, p. 95–110, doi:10.1098/rsta.1991.0109.

Le Gall, B., Ahmed Daoud, M., Rolet, J., and Moussa Egueh, N., 2011, Large-scale flexuring and antithetic extensional faulting along a nascent plate boundary in the SE Afar rift: Terra Nova, v. 23, p. 416–420, doi:10.1111/j.1365-3121.2011.01029.x.

Li, F., Dyt, C., and Griffiths, C., 2004, 3D modelling of flexural isostatic deformation: Computers & Geosciences, v. 30, p. 1105–1115, doi:10.1016/j.cageo.2004.08.005.

Makris, J., and Ginzburg, A., 1987, The Afar Depression: Transition between continental rifting and sea floor spreading: Tectonophysics, v. 141, p. 199–214, doi:10.1016/0040 -1951(87)90186-7.

McClusky, S., and 10 others, 2010, Kinematics of the southern Red Sea–Afar Triple junction and implications for plate dynamics: Geophysical Research Letters, v. 37, L05301, doi:10.1029/2009GL041127.

Montelli, R., Nolet, G., Dahlen, F.A., Masters, G., Engdahl, E.R., and Hung, S.H., 2004, Finite-frequency tomography reveals a variety of plumes in the mantle: Science, v. 303, p. 338–343, doi:10.1126/science.1092485.

Mutter, J.C., 1985, Seaward dipping reflectors and the continent-ocean boundary at passive continental margins: Tectonophysics, v. 114, p. 117–131, doi:10.1016/0040-1951(85) 90009-5.

Mutter, J.C., Talwani, M., and Stoffa, P., 1982, Origin of seaward-dipping reflectors in oceanic crust off the Norwegian margin by subaerial seafloor spreading: Geology, v. 10, p. 353–357, doi:10.1130/0091-7613(1982)10<353:OOSRIO>2.0.CO;2.

Nielsen, T.F.D., 1975, Possible mechanism of continental breakup in the North Atlantic: Nature, v. 253, p. 182–184, doi:10.1038/253182a0.

Nielsen, T.K., and Hopper, J.R., 2004, From rift to drift: Mantle melting during continental breakup: Geochemistry, Geophysics, Geosystems, v. 5, Q07003, doi:10.1029 /2003GC000662.

Nobile, A., Pagli, C., Keir, D., Wright, T.J., Ayele, A., Ruch, J., and Acocella, V., 2012, Dike-fault interaction during the 2004 Dallol intrusion at the northern edge of the Erta Ale Ridge (Afar, Ethiopia): Geophysical Research Letters, v. 39, L19305, doi:10.1029/2012GL053152.

Pagli, C., Wright, T.J., Ebinger, C.J., Yun, S.H., Cann, J.R., Barnie, T., and Ayele, A., 2012, Shallow axial magma chamber at the slow-spreading Erta Ale Ridge: Nature Geoscience, v. 5, p. 284–288, doi:10.1038/ngeo1414.

Palmason, G., 1980, A continuum model for crustal generation in Iceland: Journal of Geophysical Research, v. 47, p. 7–18.

Pérez-Gussinyé, M., Metois, M., Fernández, M., Vergés, J., Fullea, J., and Lowry, A.R., 2009, Effective elastic thickness of Africa and its relationship to other proxies for lithospheric structure and surface tectonics: Earth and Planetary Science Letters, v. 287, p. 152–167, doi:10.1026/j.epsl.2009.08.004.

Pizzi, A., Coltorti, M., Abebe, B., Disperati, L., Sacchi, G., and Salvini, R., 2006, The Wonji fault belt (main Ethiopian Rift): Structural and geomorphological constraints and GPS monitoring, *in* Yirgu, G., et al., eds., The Afar Volcanic Province within the East Afri-

can Rift System: Geological Society of London Special Publication 259, p. 191–207, doi:10.1144/GSL.SP.2006.259.01.16.

Planke, S., and Eldholm, O., 1994, Seismic response and construction of seaward dipping wedges of flood basalts: Vøring volcanic margin: Journal of Geophysical Research, v. 99, p. 9263–9278, doi:10.1029/94JB00468.

Quirk, D.G., Shakerley, A., and Howe, M.J., 2014, A mechanism for construction of volcanic rifted margins during continental breakup: Geology, v. 42, p. 1079–1082, doi:10.1130/G35974.1.

Rooney, T.O., Herzberg, C., and Bastow, I.D., 2012, Elevated mantle temperature beneath East Africa: Geology, v. 40, p. 27–30, doi:10.1130/G32382.1.

Rowland, J.R., Baker, E., Ebinger, C., Keir, D., Kidane, T., Biggs, J., Hayward, N., and Wright, T., 2007, Fault growth at a nascent slow-spreading ridge: 2005 Dabbahu rifting episode, Afar: Geophysical Journal International, v. 171, p. 1226–1246, doi:1111/j.1365–246X.2007.03584.x.

Stuart, G.W., Bastow, I.D., and Ebinger, C.J., 2006, Crustal structure of the northern Main Ethiopian Rift from receiver function studies, *in* Yirgu, G., et al., eds., The Afar Volcanic Province within the East African Rift System: Geological Society, London, Special Publication 259, p. 253–267, doi:10.1144/GSL.SP.2006.259.01.20.

Talbot, C.J., 2008, Hydrothermal salt—But how much?: Marine and Petroleum Geology, v. 25, p. 191–202, doi:10.1016/j.marpetgeo.2007.05.005.

Tard, F., Masse, P., Walgenwitz, F., and Gruneisen, P., 1991, The volcanic passive margin in the vicinity of Aden, Yemen: Bulletin des Centres de Recherches Exploration-Production Elf-Aquitaine, v. 15, p. 1–9.

ten Brink, U., 1991, Volcano spacing and plate rigidity: Geology, v. 19, p. 397–400, doi:10.1130/0091-7613(1991)019<0397:VSAPR>2.3.CO;2.

Thybo, H., and Nielsen, C., 2009, Magma-compensated crustal thinning in continental rift zones: Nature, v. 457, p. 873–876, doi:10.1038/nature07688.

Tiberi, C., Ebinger, C., Ballu, V., Stuart, G., and Oluma, B., 2005, Inverse models of gravity data from the Red Sea–Aden–East African rifts triple junction zone: Geophysical Journal International, v. 163, p. 775–787, doi:10.1111/j.1365-246X.2005.02736.x.

Turcotte, D.L., and Schubert, G., 2002, Geodynamics (second edition): Cambridge, Cambridge University Press, 456 p.

Vigny, C., Huchon, P., Ruegg, J.-C., Khanbari, K., and Asfaw, L.M., 2006, Confirmation of Arabia plate slow motion by new GPS data in Yemen: Journal of Geophysical Research, v. 111, B02402, doi:10.1029/2004JB003229.

Weissel, J.K., and Karner, G.D., 1989, Flexural uplift of rift flanks due to mechanical unloading of the lithosphere during extension: Journal of Geophysical Research, v. 94, p. 13,919–13,950, doi:10.1029/JB094iB10p13919.

Whaler, K.A., and Hautot, S., 2006, The electrical resistivity structure of the crust beneath the northern Main Ethiopian Rift, *in* Yirgu, G., et al., eds., The Afar Volcanic Province within the East African Rift System: Geological Society, London, Special Publication 259, p. 293–305, doi:10.1144/GSL.SP.2006.259.01.22.

White, R., and McKenzie, D., 1989, Magmatism at rift zones: The generation of volcanic continental margins and flood basalts: Journal of Geophysical Research, v. 94, p. 7685–7729, doi:10.1029/JB094iB06p07685.

White, R., Smith, L.K., Roberts, A.W., Christie, P.A.F., Kusznir, N.J., and the iSIMM Team, 2008, Lower-crustal intrusion on the North Atlantic continental margin: Nature, v. 452, p. 460–464, doi:10.1038/nature06687.

Wolfenden, E., Ebinger, C., Yirgu, G., Deino, A., and Ayalew, D., 2004, Evolution of the northern Main Ethiopian rift: birth of a triple junction: Earth and Planetary Science Letters, v. 224, p. 213–228, doi:10.1016/j.epsl.2004.04.022.

Wolfenden, E., Ebinger, C., Yirgu, G., Renne, P., and Kelley, S., 2005, Evolution of a volcanic rifted margin: Southern Red Sea, Ethiopia: Geological Society of America Bulletin, v. 117, p. 846–864, doi:10.1130/B25516.1.

Wright, T.J., Ebinger, C., Biggs, J., Ayele, A., Yirgu, G., Keir, D., and Stork, A., 2006, Magma-maintained rift segmentation at continental rupture in the 2005 Afar dyking episode: Nature, v. 442, p. 291–294, doi:10.1038/nature04978.

Wright, T.J., and 12 others, 2012, Geophysical constraints on the dynamics of spreading centres from rifting episodes on land: Nature Geoscience, v. 5, p. 242–250, doi:10.1038/ngeo1428.

Zanettin, B., and Justin-Visentin, E., 1975, Tectonical and volcanological evolution of the western Afar margin (Ethiopia), *in* Pilger, A., and Rosler, A., eds., Afar Depression of Ethiopia: International Union of Geodesy and Geophysics Science Report 14: Stuttgart, Germany, Schweizerbart, p. 300–309.